Control of the Fold Surface Conformation of the Lamellae of an Oligomer

ARTICLE *in* LANGMUIR · JUNE 2009

Impact Factor: 4.46 · DOI: 10.1021/la9004505 · Source: PubMed

Langmuir
Article
pubs.acs.org/Langmuir

Control of the Fold Surface Conformation of the Lamellae of an Oligomer

Yiu-Ting R. Lau,[†] Jerold M. Schultz,[‡] Lu-Tao Weng,[§] Kai-Mo Ng,[†,∥] and Chi-Ming Chan*,[†]

[†]*Department of Chemical and Biomolecular Engineering, Hong Kong University of Science and Technology, Clear Water Bay, Hong Kong,* [‡]*Department of Chemical Engineering, University of Delaware, Newark, Delaware 19716,* [§]*Materials Characterization and Preparation Facility, Hong Kong University of Science and Technology, Clear Water Bay, Hong Kong, and* [∥]*Advanced Engineering Materials Facility, Hong Kong University of Science and Technology, Clear Water Bay, Hong Kong*

Received February 5, 2009. Revised Manuscript Received April 19, 2009

Small-angle X-ray scattering revealed that a semirigid oligomer of bisphenol-A-*co*-ether-octane with a monodisperse chain length is capable of forming ciliated-folded, once-folded, ciliated-extended and fully extended lamellar structures. Isothermal crystallization studies suggested a sequence of structures with increasing crystallization temperature, from a ciliated-folded to a once-folded form and then to a ciliated-extended form as the degree of supercooling is decreased. The crystal surface thus changed from octane cilia to bisphenol A segments and then back to octane cilia as the lamellar structure changed. The results of time-of-flight secondary ion mass spectrometry analyses strongly supported the fold structural models.

Introduction

Chain-folded crystal structure of polymers is regarded as a morphological metastable state as a consequence of the counteraction between the thermodynamic equilibrium and the kinetics barrier to the increase in the lamellar thickness.[1] As generalized in the classical Gibbs−Thomson equation, the lamellar thickness in association with the melting temperature of polymer crystals is kinetic in origin.[2] The relationship between the lamellar thickness and metastability can be illustrated from a number of crystallization studies on oligomers, such as *n*-alkanes,[3] ethyleneoxides,[4] hydroxybutyrates,[5] nylon amides,[6] and phenylene sulfides,[7] with the attempt to locate the onset chain length for crystal folding to occur. The fold stability is intuitively determined by the differences between the intramolecular forces due to the attractive interaction between polymer segments upon chain folding, and the energies used to overcome the torsion-angle and bond-angle deformations.[8] A polymer chain may adopt an integer form of lamellar structures such that the chain ends and structural defects are effectively expelled to the fold surfaces. The lamellae may transiently occur as noninteger folded (NIF) forms and gradually transform to chain-extended or integer folded (IF) forms by thermal annealing at a particular supercooling.[9] Such quantized fashion of crystallization paves the way for manipulating the lamellar thickness of polymer crystals via cocrystallization,[10] modification of the end groups,[11] and incorporation of chain architectural defects.[9a,12]

Switchboard and adjacent reentry are generally the two accepted models to portray how the chain molecules fold on the lamellar surface of a polymer crystal.[13] There have been very strong debates and discussions on which model is the correct model to describe the fold structures of polyethylenes based on the empirical data of neutron scattering[14] and infrared spectroscopy.[15] It is yet reasonable to anticipate that the oligomers with short chain lengths take the latter pathway so that they are able to form some integer form lamellar structures.[3] Most homogeneous systems that have been reported to have the feature of integral folding are homopolymers, such as polyethylene and poly(ethyleneoxide), and hardly have we found any significant difference in the polymer structures to distinguish the fold surfaces from the lateral crystalline portions of the lamellae. Atkins and co-workers have ever raised a question about the chemical nature of folds in one of their follow-up papers on the crystal structures of oligoamides.[16] They suggested that both the amide and short alkane unit were plausibly used as the folds of the lamellae such that the chosen fold conformation was commensurate with the hairpin

*To whom correspondence should be addressed.

(1) Cheng, S. Z. D.; Keller, A. *Annu. Rev. Mater. Sci.* **1998**, *28*, 533–562.
(2) Hoffman, J. D.; Davis, G. T.; Lauritzen, J. I., In *Treatise on Solid State Chemistry: Crystalline and Noncrystalline Solids*; Hannay, N. B., Ed.; Plenum Press: New York, 1976; Vol. *3*, pp 497−614.
(3) Ungar, G.; Stejny, J.; Keller, A.; Bidd, I.; Whiting, M. C. *Science* **1985**, *229*, 386–389.
(4) (a) Hoffman, J. D. *Macromolecules* **1986**, *19*, 1124–1128. (b) Buckley, C. P.; Kovacs, A. J., In *Structure of Crystalline Polymers*; Hall, I. H., Ed.; Elsevier: London, 1984; pp 261−307.
(5) Li, J.; Organ, S. J.; Hobbs, J. K.; Terry, A. E.; Barham, P. J.; Seebach, D. *Polymer* **2004**, *45*, 8913–8923.
(6) Cooper, S. J.; Atkins, E. D. T.; Hill, M. J. *Macromolecules* **1998**, *31*, 8947–8956.
(7) Fagerburg, D. R.; Watkins, J. J.; Lawrence, P. B. *Macromolecules* **1993**, *26*, 114–118.
(8) Sundararajan, P. R.; Kavassalis, T. A. *J. Chem. Soc., Faraday Trans.* **1995**, *91*, 2541–2549.
(9) (a) Ungar, G.; Zeng, X. B.; Brooke, G. M.; Mohammed, S. *Macromolecules* **1998**, *31*, 1875–1879. (b) Cheng, S. Z. D.; Zhang, A.; Barley, J. S.; Chen, J. H.; Habenschuss, A.; Zschack, P. R. *Macromolecules* **1991**, *24*, 3937–3944. (c) Organ, S. J.; Li, J.; Terry, A. E.; Hobbs, J. K.; Barham, P. J. *Polymer* **2004**, *45*, 8925–8936.
(10) Hosier, I. L.; Bassett, D. C. *J. Polym. Sci., Part B: Polym. Phys.* **2001**, *39*, 2874–2887.
(11) (a) Booth, C.; Domszy, R. C.; Leung, Y. K. *Makromol. Chem.* **1979**, *180*, 2765–2767. (b) Cheng, S. Z. D.; Wu, S. S.; Chen, J. H.; Zhuo, Q.; Quirk, R. P.; Von Meewall, E. D.; Hsiao, B. S.; Habenschuss, A.; Zschack, P. R. *Macromolecules* **1993**, *26*, 5105–5117.
(12) (a) De Ten Hove, C. L. F.; Penelle, J.; Ivanov, D. A.; Jonas, A. M. *Nat. Mater.* **2004**, *3*, 33–37. (b) Schuurmans, N.; Uji-i, H.; Mamdouh, W.; De Schryver, F. C.; Feringa, B. L.; van Esch, J.; De Feyter, S. *J. Am. Chem. Soc.* **2004**, *126*, 13884–13885.
(13) Peterlin, A. *Macromolecules* **1980**, *13*, 777–782.
(14) (a) Sadler, D. M.; Keller, A. *Macromolecules* **1977**, *10*, 1128–1140. (b) Yoon, D. Y.; Flory, P. J. *Polymer* **1977**, *18*, 509–513. (c) Hoffman, J. D.; Guttman, C. M.; DiMarzio, E. A. *Faraday Discuss. Chem. Soc.* **1979**, *68*, 177–197.
(15) Cheam, T. C.; Krimm, S. *J. Polym. Sci., Polym. Phys. Ed.* **1981**, *19*, 423–447.
(16) Atkins, E. D. T.; Hill, M. J.; Jones, N. A.; Sikorski, P. *J. Mater. Sci.* **2000**, *35*, 5179–5186.

Scheme 1. Molecular Structure of Monodisperse Oligomer of BA-C8-3

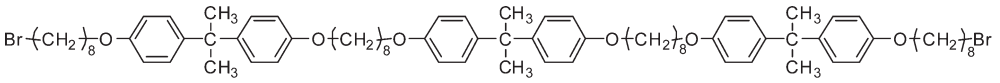

symmetry in integer form folding and the saturation of hydrogen bonds. However, there was no definitive proof to disclose the difference in the fold chemical structures, and whether these changes in the fold nature produce any significant impact on the unit cell dimensions is controversial.

In this contribution, we report on a simple methodology to control the fold structural conformation at the crystal surfaces by maneuvering the development of all the possible lamellar structures that can be obtained from an oligomeric material. We reveal for the first time that the chemical structure of the fold of the monodisperse oligomer of bisphenol-A-*co*-ether-octane, which consists of rigid and flexible segments, can be controlled through changes in the crystallization temperature. We hope that this work may ultimately lead to a greater understanding of the structural relationship between the fold surface and the crystalline portion of chain-folded lamellae of polymers.

Experimental Section

Bisphenol-A-*co*-ether-octane with a monodisperse chain length of three repeat units, designated as BA-C8-3, was synthesized by a routine process that involved functional group protections, condensation reactions, and functional group deprotections based on the starting monomers of 8-bromooctanol, bisphenol A, and 2-methoxyethoxymethyl-monocapped bisphenol A (see Supporting Information). The structure of the molecule is shown as Scheme 1.

Films with thicknesses of 100−200 μm were prepared by casting a concentrated chloroform solution of the oligomers onto Kapton tapes. The solvent was allowed to evaporate slowly at room temperature in a fume hood. After solvent evaporation, they were held at 90 °C for about 15 min. Then the melt films were quenched and annealed isothermally at a chosen crystallization temperature on a hot stage. The small-angle X-ray scattering (SAXS) measurements were performed with an evacuated SAXS instrument SAXSess (Anton Paar GmbH, Austria) equipped with a one-dimensional (1D) elliptical focusing graded multilayer mirror, Kratky compact camera, and block-collimating unit, which is able to produce monochromatic Cu Kα X-rays (40 kV, 50 mA). The scattered X-ray intensities were detected by a two-dimensional (2D) imaging plate, which had a spatial resolution of $42.3 \times 42.3\,\mu m^2$ per pixel. The desmearing procedure of the image was performed using SAXSQuant software from Anton Paar by measurement of the primary beam cross-section profiles (beam width and beam length). The scattering data were then corrected for the sample absorption of the X-rays and transformed to the q-scale.

Results and Discussion

Figure 1 shows SAXS scans for BA-C8-3 samples crystallized at different temperatures. The SAXS scans were all made at room temperature. Most of the metastable and stable crystalline forms were successfully identified from the SAXS profiles of the samples prepared by melt-crystallization. Four major peaks were identified, at $q = 0.93$, 1.04, 1.88, and 2.13 nm^{-1}, corresponding to long periods of 6.73, 6.06, 3.34, and 2.95 nm, respectively, based on the equation $d \approx 2\pi/q$, where d is the Bragg spacing and q is the scattering vector defined by $q = 4\pi/\lambda \sin(\theta/2)$, in which λ is the wavelength of the X-rays and θ is the angle between the incident beam and the scattered radiation. Although it is tempting to assign Peaks 2 and 4 as second orders of Peaks 1 and 3, time-of-flight secondary ion mass spectrometry (ToF-SIMS) results, shown later, dictate that Peaks 2 and 4 must be first-order peaks of structures different from those represented by Peaks 1 and 3. Given that Peaks 1−4 represent different structures, those structures are reasonably given as follows. Peak 1, with a long period of 6.73 nm, is characteristic of a chain-extended lamellar structure (c.f., Structure 1 in Figure 1) since this value is close to the predicted end-to-end distance of an energy-minimized extended structure of a freely bound chain. The end-to-end length of an extended BA-C8-3 chain is determined to be 6.88 nm by a molecular modeling software (Accelrys Materials Visualizer). The other peaks are assigned to the characteristic lamellar structures shown in Figure 1. Notably, the long period of Peak 3 is one-half of that determined from Peak 1, and it is most possibly represented by a once-folded structure (c.f., Structure 3 in Figure 1). Peaks 2 and 4, which are nearly shouldered on the first and third peaks, respectively, are proposed to be the kinetic forms of the once-folded and the chain-extended structures. Structure 2 (the ciliated-extended structure), with a lamellar thickness slightly less than that of the fully extended structure (Structure 1), is associated with Peak 2. Structure 4 (the ciliated-folded structure), with a lamellar thickness slightly less than that of the once-folded structure (Structure 3), is associated with Peak 4.

Figure 1 shows that, in addition to the most stable chain-extended lamellar structure (Structure 1), which was present at all temperatures between 35 and 75 °C, other ordered structures were also produced at different temperatures. Structures 3 and 4, which are not the most energetically favorable structures, are metastable structures because of the folding of the chains. The metastable Structure 4, which was formed at 35 °C, became supplanted by another metastable Structure 3 at higher crystallization temperatures, as indicated by the near disappearance of Peak 4 and the appearance of Peak 3 at 46 °C and the total disappearance of Peak 4 at 60 °C, as shown in Figure 1. Eventually, only the most stable chain-extended structure existed after crystallization at 75 °C. The appearance and disappearance of the metastable structures must change the chemical structure of the fold surface of the crystals. Such changes were detected using ToF-SIMS, as shown later.

To validate the SAXS results, we monitored the isothermal melt crystallization of BA-C8-3 as a function of the degree of supercooling with a differential scanning calorimeter (DSC). We aimed to observe the transitions between the metastable and stable lamellar structures detected by SAXS. Figure 2a shows DSC scans for specimens crystallized at different temperatures. In Figure 2a, Peak 1 is reasonably assumed to be the equilibrium melting temperature of the fully extended crystal (T_m^o = 85 °C) because this peak (reflecting the extended chain structure) is invariant with crystallization temperature (T_c). These crystals can be grown even when T_c is moved closer to the melting point. When T_c was equal to or lower than 65 °C, an additional, lower-temperature endotherm is observed. The lower-temperature endotherm is followed immediately by an exotherm, indicating that, when the original crystals, which are of low stability, melt, they recrystallize into a structure of greater stability. DSC scans run at increasing heating rates confirm that the highest-temperature peak cannot be fully produced in the recrystallization process. These results are given in Figure 2b. Even at the highest heating rate, at which the recrystallization process must be

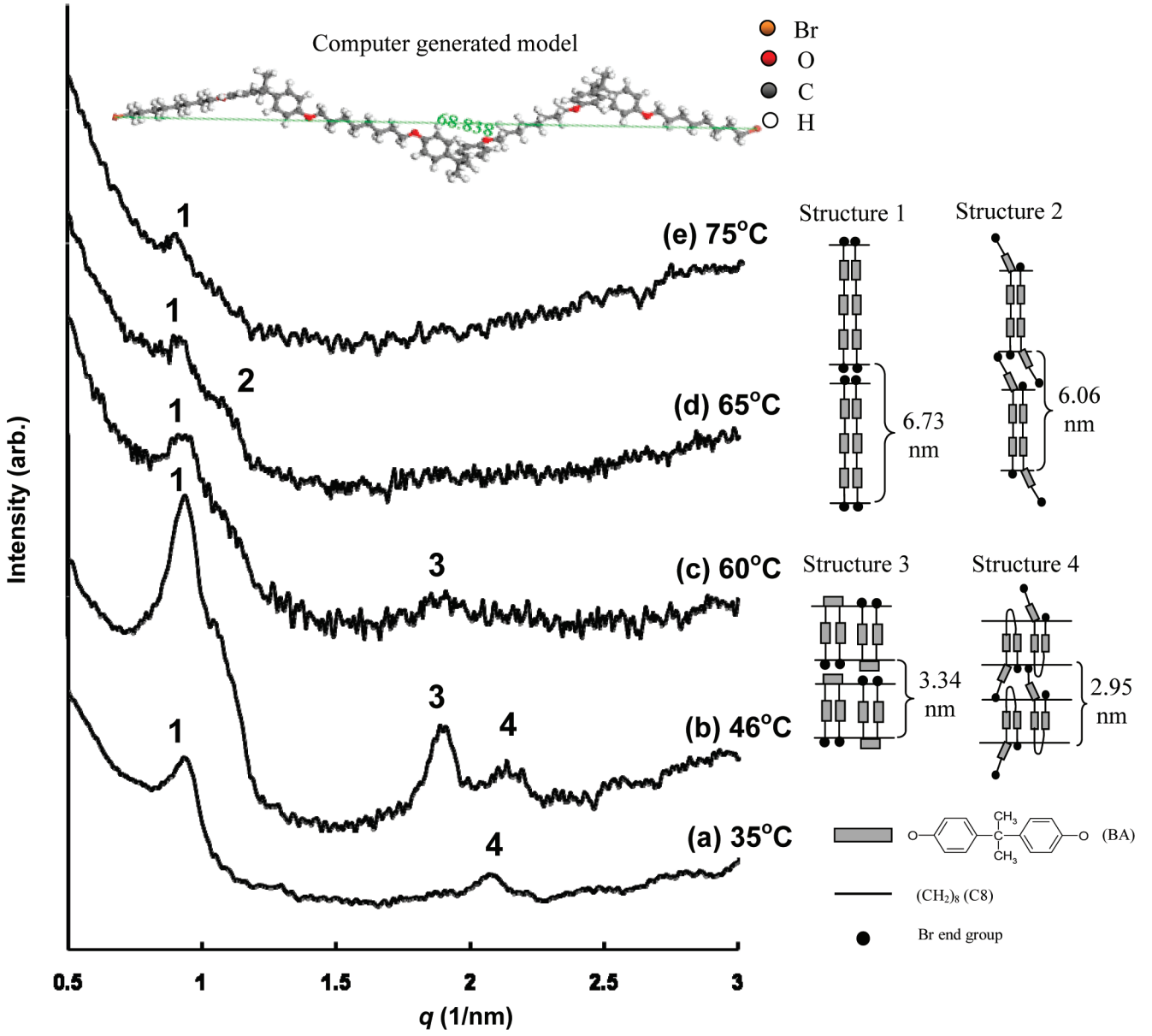

Figure 1. Desmeared scattering profiles of bulk crystallized films of BA-C8-3 samples obtained at different temperatures (a−e). The insets show the proposed structures with measured lamellar thicknesses and a computer model of a fully extended structure of a freely bound BA-C8-3 chain at its lowest energy state. The end-to-end distance of the simulated model was determined to be 68.838 Å (6.88 nm).

retarded, the highest-temperature peak is unaffected. In Figure 2a, three peaks, which are labeled as Peaks 2, 3, and 4 on the thermograms, are associated with Structures 2, 3, and 4, respectively (Figure 1), based on the peak temperatures. The gradual movement of Peak 4 (c.f., Structure 4 in Figure 1), which is originally located at 58 °C, to high temperatures to eventually become Peak 3 (c.f., Structure 3 in Figure 1) at 63 °C suggests a shift from the ciliated-folded form (Structure 4) to the once-folded form (Structure 3). Crystallization at 65 °C exhibits an endotherm, labeled 2, at 80 °C. Endotherm 2 likely represents melting of the ciliated-extended form, in agreement with the SAXS results of Figure 1.

The DSC results for material crystallized at 35 °C and at 60 °C require additional comment. The SAXS results show that the dominant form produced by crystallization at 35 °C is Structure 4. On the other hand, the melting signature of Structure 3 (a small endotherm at 63 °C) appears in the DSC scan. It appears that this endotherm has been created through recrystallization of Structure 4. The SAXS results of Figure 1 show that Structure 3 can develop directly during crystallization at 60 °C, but not at higher temperatures. The exotherm at 60 °C for material crystallized at 35 °C would be the crystallization of Structure 3 from the molten remnant of Structure 4. For material crystallized at higher temperatures, the higher melting temperatures (> 60 °C) of the apparently more perfect forms of Structure 4 are too high to allow crystallization of Structure 3. Between crystallization temperatures of 40 and 60 °C, the crystals formed appear to gradually assume more of the character of Structure 3, culminating in crystallization directly into Structure 3 at 60 °C.

For material crystallized at 60 °C, two exotherms are observed, at approximately 67 and 72 °C. In this DSC scan, one also observes a small endothermic peak at 80 °C, which corresponds to Structure 2. Hence, the two exotherms involve two possible nonisothermal recrystallizations from Structure 3 to Structure 2 and from Structure 3 to Structure 1. In order to verify that the exotherm is related to a possible transformation, we first heated a specimen initially crystallized at 40 °C to a temperature just above its exothermic peak and equilibrated at this temperature. This is

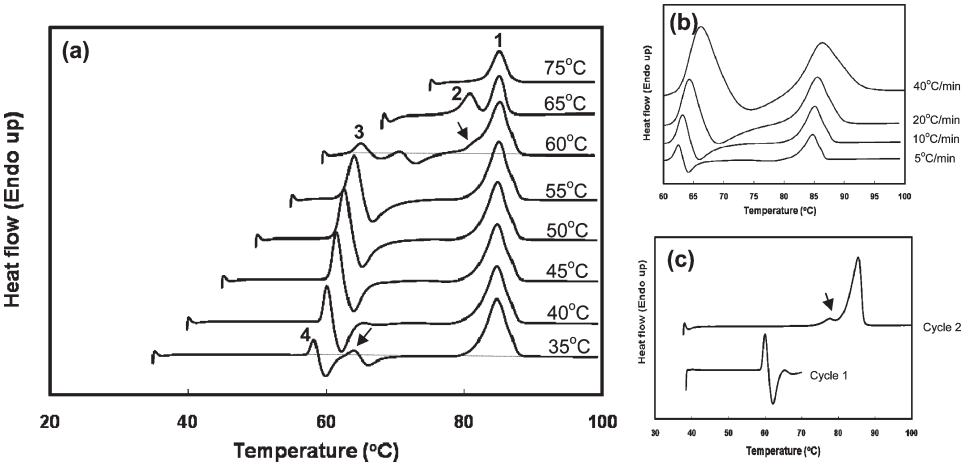

Figure 2. (a) Subsequent heating thermograms (PerkinElmer Diamond DSC) of BA-C8-3 after isothermal melt crystallization to equilibrium states at temperatures from 40 to 75 °C. The heating rate was 10 °C min^{-1}. The dotted lines indicate the baselines of the thermograms for clarity. (b) The influence of heating rates (from 5 to 40 °C min^{-1}) on subsequent heating thermograms after isothermal melt crystallization at the selected temperature of 55 °C. (c) Subsequent heating thermograms of BA-C8-3 that was isothermally crystallized at 40 °C in the first cycle and that of BA-C8-3 after being allowed to recrystallize at 70 °C in the second cycle. In Cycle 1, the crystallized sample at 40 °C was heated to 70 °C at the rate of 10 °C min^{-1} and equilibrated at 70 °C. The sample was then cooled to 40 °C and heated at the same rate of 10 °C min^{-1} to 100 °C in Cycle 2. The arrows indicate the small endothermic peaks due to recrystallization processes upon thermal heating.

shown as Cycle 1 in Figure 2c. After cooling to 40 °C, another scan was made, to 100 °C (Cycle 2). The endotherm at 80 °C shows that the metastable structures originally produced at 40 °C can be partly transformed to Structure 2 via recrystallization. The combination of SAXS and DSC results align with the proposed sequence of the lamellar structures as a function of crystallization temperature given in Figure 3.

The above discussions are in line with results of lamellar transformation of sharp fractions of other oligomers, such as *n*-alkanes,[3] ethyleneoxides,[4] hydroxybutyrates,[5] and nylon amides.[6] The transformation of a metastable NIF form to the chain-extended or IF form has been observed upon annealing.[9]

It should be noted that the above analyses do not provide direct evidence on the structures of the folds. In addition, the SAXS results do not provide an unequivocal proof that Peaks 3 and 4 are not the second-order scattering of Peaks 1 and 2, respectively. ToF-SIMS, which is an extremely surface-sensitive technique, has been widely used for differentiation and quantification of various polymer structures.[17] We have successfully utilized this surface-sensitive technique to investigate the surface segregation of end groups and low-energy components on the surfaces of lamellae.[18] Here, we used ToF-SIMS to investigate the fold surfaces of the lamellae of BA-C8-3, with the objective of producing chemical evidence that can be used to support the hypothesis that Peaks 3 and 4 are not the second-order scattering of Peaks 1 and 2, respectively. We prepared solutions of BA-C8-3 at a concentration of 20−40 mg cm^{-3} in chloroform. These solutions were used to spin-coat 100- to 300-nm-thick films on preheated SiO_2 substrates. The melt-coated substrates were sealed in glass tubes, which were quenched in liquid nitrogen. The polymer films were then crystallized at various temperatures in a ventilated oven under a nitrogen purge. High-resolution mass spectra were obtained under an ultrahigh vacuum (1.5×10^{-9} torr) from a Physical Electronics PHI 7200 ToF-SIMS spectrometer, using Cs^+ as the primary ion source

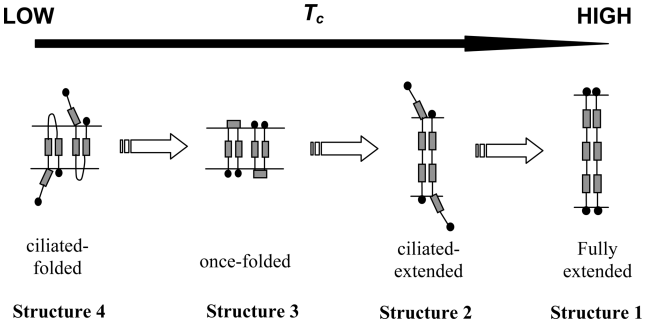

Figure 3. Schematic showing the structural transformation as a function of crystallization temperature (T_c).

operated at 8 keV. The total ion dose was lower than 4×10^{11} ions cm^{-2}.

In our previous studies, we showed that the surfaces of edge-on and flat-on lamellae of poly(bisphenol-A-*co*-ether-octane) could be differentiated by ToF-SIMS using ions that are characteristic of different polymer segments.[19] The matrix effect on the composition quantification was also shown to be negligible, from the intensity ratios between any two characteristic ions from the spectra based on the following equation: $R_{j/k} = I_j/I_k$, where I is the absolute intensity of an ion fragment at the mass-to-charge ratio (m/z) = j or k. Three characteristic molecular ions at m/z = 111, 135, and 325 were chosen from the positive spectra. They are characteristic of the octane segments, bisphenol A segments and the cilium segments, respectively. Figure 4a presents a typical atomic force microscopy (AFM) height image of a 250-nm thick BA-C8-3 film crystallized at 60 °C obtained with a Nanoscope III Multimode AFM (Digital Instruments). Nanoprobe silicon tips with a resonance frequency of approximately 300 kHz and a spring constant of about 40 Nm^{-1} were used. The AFM results show that all samples prepared for the ToF-SIMS analyses had flat-on lamellae at the surface. The molecular structures of the selected ions used to calculate $R_{j/k}$ are shown in Figure 4b,c. In Figure 4b, $R_{j/k}$ represents the ratio of the concentration of the

(17) Chan, C. M. *Polymer Surface Modification and Characterization*, 1st ed.; Hanser Publishers: New York, 1994, pp 153−192.

(18) (a) Li, L.; Ng, K. M.; Chan, C. M.; Feng, J. Y.; Zeng, X. M.; Weng, L. T. *Macromolecules* **2000**, *33*, 5588–5592. (b) Lei, Y. G.; Cheung, Z. L.; Ng, K. M.; Li, L.; Weng, L. T.; Chan, C. M. *Polymer* **2003**, *44*, 3883–3890. (c) Cheung, Z. L.; Weng, L. T.; Chan, C. M.; Hou, W. M.; Li, L. *Langmuir* **2005**, *21*, 7968–7970.

(19) Lau, Y. T. R.; Weng, L. T.; Ng, K. M.; Chan, C. M. *Appl. Surf. Sci.* **2008**, *255*, 1001–1005.

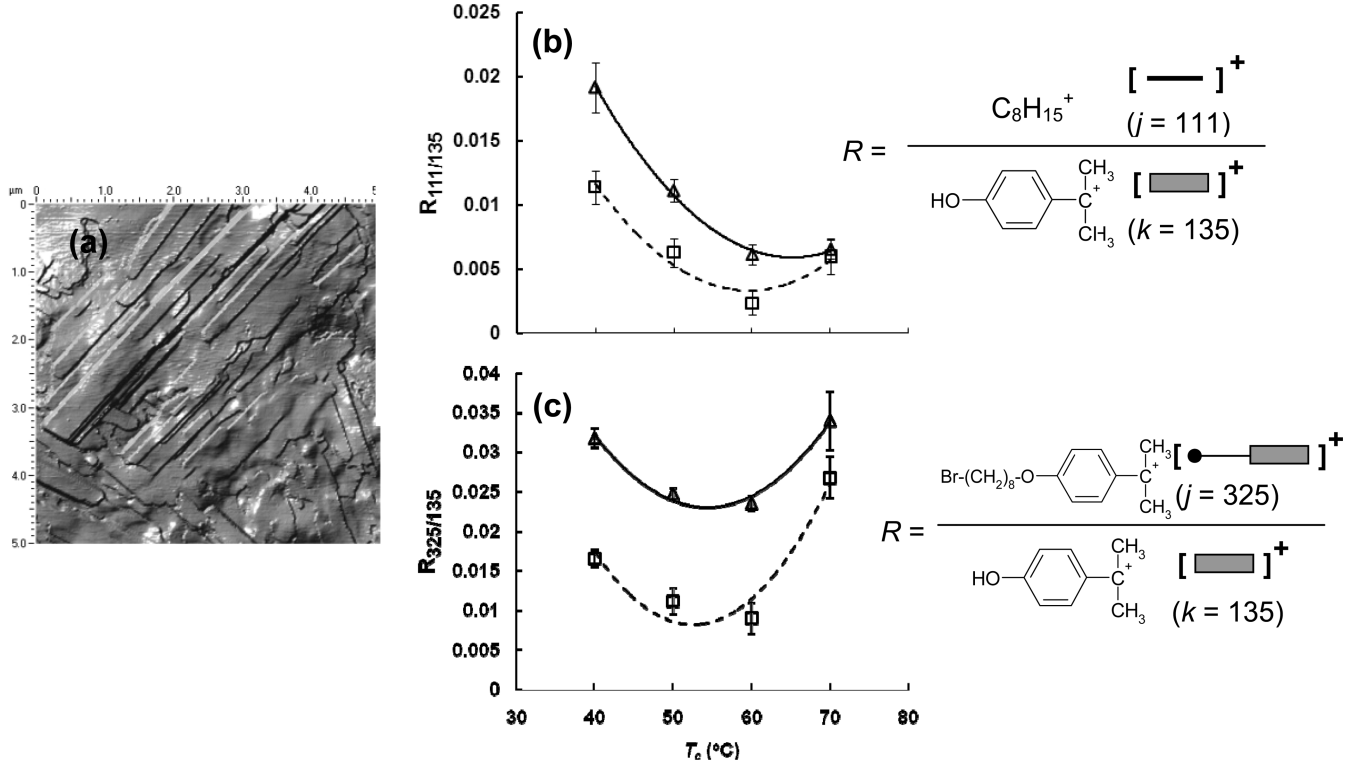

Figure 4. (a) AFM height image of the surface morphology of a BA-C8-3 film (with an initial thickness of 250 nm) crystallized at a temperature of 60 °C. (b) The plot of $R_{j/k}$ (j = 111 and k = 135) versus the crystallization temperature (T_c) of films with thicknesses of 150 nm (□) and 250 nm (Δ). (c) The plot of $R_{j/k}$ (j = 325 and k = 135) versus the crystallization temperature (T_c) of films with thicknesses of 150 nm (□) and 250 nm (Δ).

octane segments to that of the bisphenol A segments, and in Figure 4c, $R_{j/k}$ represents the ratio of concentration of the cilium segments to that of the bisphenol A segments. At crystallization temperatures below 60 °C, the $R_{j/k}$ values decreased as the crystallization temperature increased, indicating that the concentrations of the cilium and octane segment on the crystal surfaces decreased as a result of the supplanting of the ciliated-folded structure by the once-folded structure and that the concentration of the once-folded structure increased with crystallization temperature. For crystallization temperatures above 60 °C, the cilium concentration increased, due to the supplanting of the once-folded structure by the ciliated-extended structure. Similar results were observed from samples of two different film thicknesses, indicating the absence of film thickness effects. If Structures 3 and 4 do not exist, following the hypothesis stating that Peaks 3 and 4 in the SAXS curves are the second-order scattering of Peaks 1 and 2, respectively, then we should not expect that the surface chemical composition of the crystals be changed as a function of crystallization temperature. However, the ToF-SIMS results have provided strong chemical evidence that the chemical nature of the crystal surfaces did change as a function of temperature. The agreement among SAXS, DSC, and ToF-SIMS results clearly infers that lamellar folding changes occur as the crystallization temperature is increased, following the sequence displayed in Figure 3.

Conclusion

In summary, we have successfully demonstrated a simple, viable physical method to manipulate the fold surface properties of the lamellae by controlling the crystallization temperature. Future work will explore this temperature-modulated, switchable fold behavior to develop new polymeric materials with crystallizable functional moieties for surface-related applications.

Acknowledgment. We thank Prof. Subbu S. Venkatraman from the School of Materials Science and Engineering at the Nanyang Technological University for his assistance in the use of the SAXS instrument to analyze our crystallized samples. This work was supported by the Hong Kong Research Grants Council under Grant Numbers 600408 and 600405.

Supporting Information Available: Reaction and purification procedures for the synthesis of the monodisperse oligomer of BA-C8-3 with bromine end groups. This material is available free of charge via the Internet at http://pubs.acs.org.